Note: This is a preprint of a paper submitted for publication. Contents of this paper should not be quoted or referred to without permission of the author(s).

To be presented at the 1993 International Workshop on Superconductivity, Hakodate, Japan, June 28–July 1, 1993 and published in *Proceedings*

HIGH-RESOLUTION Z-CONTRAST IMAGING AND HOLE CONCENTRATION MAPPING OF YBCO THIN FILMS

S. J. Pennycook, N. D. Browning, M. F. Chisholm, S. Zhu, R. Feenstra, D. P. Norton, and D. H. Lowndes
Solid State Division
Oak Ridge National Laboratory
Oak Ridge, Tennessee 37831-6030

SOLID STATE DIVISION
OAK RIDGE NATIONAL LABORATORY
Managed by
MARTIN MARIETTA ENERGY SYSTEMS, INC.
under
Contract No. DE-AC05-84OR21400
with the
U.S. DEPARTMENT OF ENERGY
Oak Ridge, Tennessee

May 1993

MASTER

HIGH-RESOLUTION Z-CONTRAST IMAGING AND HOLE CONCENTRATION MAPPING OF YBCO THIN FILMS

S. J. Pennycook, N. D. Browning, M. F. Chisholm, S. Zhu, R. Feenstra,
D. P. Norton, and D. H. Lowndes

Solid State Division, Oak Ridge National Laboratory, Oak Ridge, Tennessee 37831-6030

ABSTRACT

Atomic-resolution Z-contrast electron microscopy provides a directly interpretable image showing the location of high-Z atomic columns without the need for any structural models. Usually, the type of column may be identified from its intensity, and the structure and morphology of interfaces, ultrathin films, and superlattices are directly revealed. This has generated many insights into growth and relaxation phenomena. Since the Z-contrast image uses only electrons scattered through large angles, electron energy loss spectroscopy may be performed simultaneously using the transmitted beam, providing information on the local hole concentration from the fine structure of the oxygen-K absorption edge. The resolution achieved is below the coherence length, allowing a microscopic interpretation of transport properties.

1. ATOMIC RESOLUTION IMAGING AND SPECTROSCOPY WITH A STEM

Figure 1 shows schematically how an atomic-resolution Z-contrast image may be formed in a high-resolution scanning transmission electron microscope (STEM) [1–3]. A thin crystalline specimen, oriented to a low-order zone axis, is scanned by a fine (coherent) probe focused to a diameter less than the spacing between the atomic columns. The electron probe is effectively channeled along each individual atomic column in turn. Part of the beam is scattered through large angles, and detected with an annular detector to form the Z-contrast image. Since the scattering cross section is approximately proportional to Z^2, where Z is atomic number, strong compositional sensitivity is achieved. Furthermore, the image shows no reversals of contrast with microscope focus or specimen thickness, which allows direct interpretation without the need for any prior structural models (see Fig. 2).

Oxygen ($Z = 8$) obviously cannot be detected in the Z-contrast image in the presence of the heavy elements Ba ($Z = 56$), Y ($Z = 39$), and Cu ($Z = 29$). However, it can be detected by electron energy loss spectroscopy (EELS), and in fact the K-edge fine structure provides a sensitive measure of local hole concentration [4]. As shown in Fig. 1, the STEM geometry allows both signals to be detected simultaneously, so that the higher intensity Z-contrast image may be used to position the probe on selected individual atomic columns for EELS. Again, the probe may be considered to channel down individual atomic columns, and using a high sensitivity, CCD-based, parallel detection system [5], atomic-resolution chemical analysis has recently been demonstrated in a semiconductor system [6]. Thus, we are in a position to correlate the atomic structure revealed in the image with local hole concentrations obtained at a scale below the coherence length.

2. CELL-BY-CELL GROWTH AND AMORPHIZATION

If all components are supplied simultaneously and stoichiometrically to a suitable substrate, YBCO grows unit cell by unit cell as shown by the observation of RHEED oscillations [7]. The underlying reason for this behavior can be deduced from Fig. 3, which shows an amorphous/crystalline interface formed by ion implantation [8]. Apart from the fact that the interface is atomically abrupt, indicative of a first order phase transition, the interface is clearly seen to be preferentially located at the Cu chain plane, stepping occasionally by complete unit cells. Since the end-of-range damage region during ion implantation is close to thermal equilibrium, this is striking evidence that the Cu-chain plane is the thermodynamically preferred crystal termination plane. YBCO therefore prefers $c\perp$ growth, and clear evidence for $c\perp$ cell-by-cell growth is seen in the images of single unit cell superlattices seen in Fig. 4 [8].
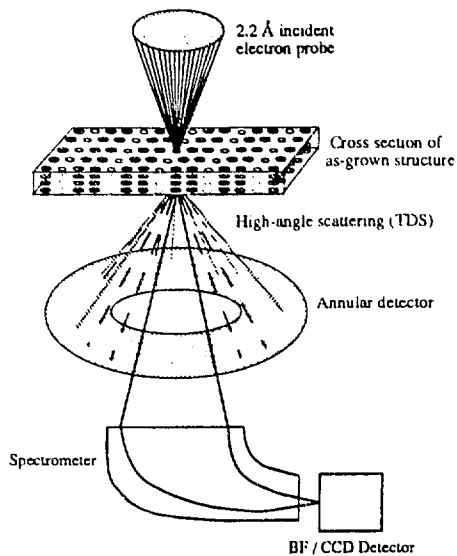
Fig. 1. Atomic-resolution incoherent imaging and analysis in the STEM. The Z-contrast image is obtained with an annular detector (typical inner semiangle 75 mrad), while electrons passing through the inner hole are used for EELS (typical collection semiangle 30 mrad).
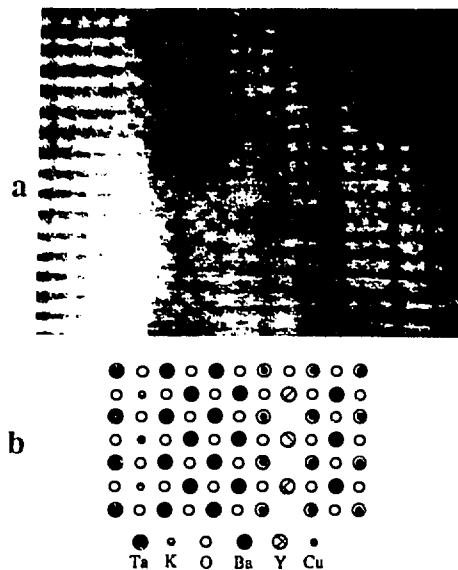

Fig. 2. (a) Unexpected transition zone seen at the interface between a YBCO film and a KaTaO$_3$ substrate. (b) The suggested structure is BaTaO$_3$, which is unstable in bulk but probably stabilized by oxygen vacancies.
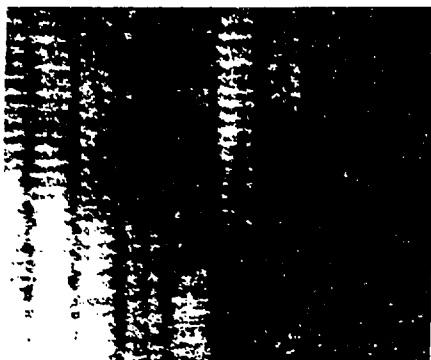

Fig. 3. Cell-by-cell amorphization observed after low-temperature oxygen ion implantation. The amorphous/crystal interface preferentially locates at the Cu-chain plane.
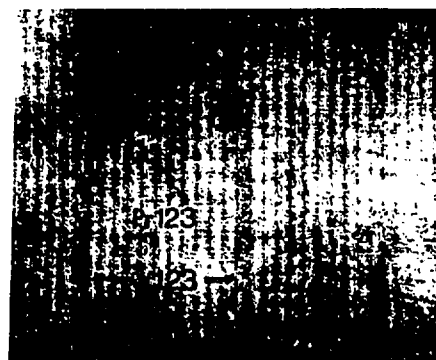

Fig. 4. Cell-by-cell growth recorded in the microstructure of a c⊥ YBCO/PrBCO superlattice. The single unit cells of YBCO frequently jump by 1 unit cell in the c direction.

At high deposition rates, a transition to the kinetically more efficient a⊥ growth has been observed. This is accompanied by significant microscopic roughness due to the shorter surface diffusion lengths [9]. Attempts to recrystallize ion-implanted YBCO by oxygen annealing at low partial pressure have also resulted in a predominantly a⊥ microstructure, again due to the short diffusion lengths available in the amorphous/crystalline interface [10]. Apart from kinetics alone, the substrate may also play a role by preferentially nucleating an a⊥ orientation; this has been observed in the case of LaAlO$_3$ [11]. Note that with an MgO substrate, two different interface structures have been observed [9], both in the c⊥ orientation. One shows localized interface dislocations indicative of strong film/substrate bonding [Fig 5(a).]. The

other shows Moire fringes indicating that the film has relaxed, even in areas only a single unit cell in thickness [Fig. 5(b)], but no interface dislocations are seen. In these regions, there can only be weak interfacial bonding.
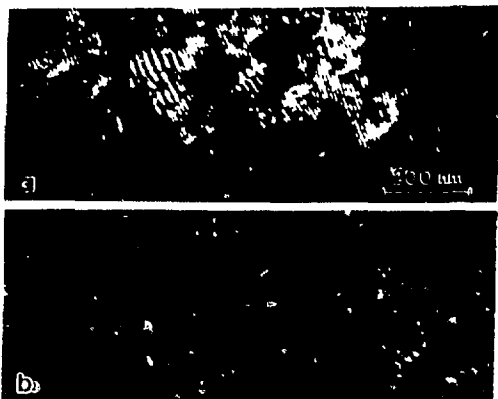

Fig. 5. (a) Plan view dark field image of a nominally 3 unit cell film of YBCO deposited on MgO. The film has formed relaxed islands showing regions of Moire fringes (fine fringes) and interfacial dislocations (wide fringes). (b) Tilted image showing only interfacial dislocations.

3. HOLE CONCENTRATION MAPPING

Sensitive measurement of local hole concentration can be obtained from the pre-edge feature on the O-K absorption edge. Careful calibration with bulk samples of known oxygen concentration indicates that δ in $YBa_2Cu_3O_{7-\delta}$ may be measured to an accuracy of approximately 5% [4]. With the VG Microscopes HB501UX STEM equipped with a sensitive parallel EELS system, these measurements may be achieved on a scale below the coherence length, in principle with the same resolution as the image itself. Equally important, a time sequence may be taken to test for beam damage or oxygen loss in the specimen during analysis. If no such effects are seen, the spectra may be added to improve statistics.

Figure 6 shows Z-contrast images of two grain boundaries in a polycrystalline film of YBCO on a YSZ substrate [12]. These films are strongly c⊥ textured, though containing many high-angle tilt grain boundaries. The tilts are close to pure (001) tilts, but not close enough to enable zone axis images to be obtained from both grains simultaneously. The a-b planes can be well resolved in both grains, and clearly show the presence of structural disorder close to the asymmetric boundary. This disorder is either due to lattice strain or a narrow amorphous zone. In contrast, the symmetric boundary shows no structural disorder at the grain boundary. Hole concentration profiles across the two boundaries are compared in Fig. 7. The symmetric boundary shows no evidence of any hole depletion, whereas the asymmetric boundary shows a deep cusp in hole concentration that extends over 50 Å either side of the boundary, much further than the range of structural disorder. We believe this observation [12] provides the first microscopic evidence that not all high-angle grain boundaries act as weak links [13].

It should be noted that the behavior of small-angle grain boundaries can be well understood on the basis of the extreme sensitivity of YBCO to the strain fields of the grain boundary dislocations [14]. The behavior of high-angle boundaries cannot be so easily modeled, and the ability to correlate the atomic structure with its effects on hole concentration is likely to prove very useful in understanding the role of defects and interfaces on macroscopic transport characteristics.

4. FUTURE DIRECTIONS

Combining atomic-resolution imaging and spectroscopy on a single microscope appears to be a very powerful method for characterizing the structure, composition, and hole doping properties of defects and interfaces, without the need for any prior knowledge or model structures. At the time of writing, a 300-kV STEM is being installed, which will increase the Z-contrast image resolution to 1.4 Å. The Cu columns in the high-T_c materials will then be clearly visible, significantly enhancing our ability to directly interpret images of defects and interfaces.
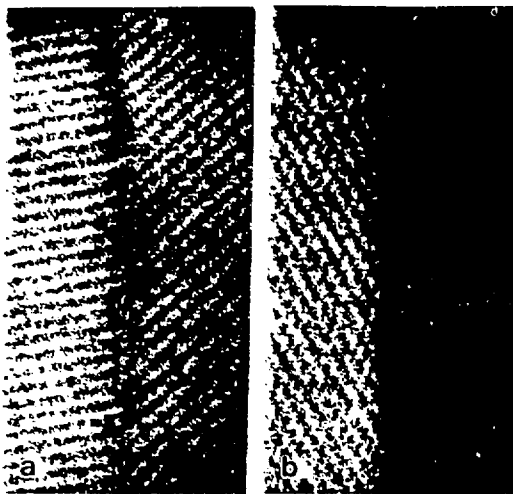
Fig. 6. Two tilt grain boundaries in poly-
crystalline YBCO deposited on YSZ.
(a) Asymmetric 29° (near Σ17) grain
boundary showing structural disorder
close to the boundary. (b) Symmetric
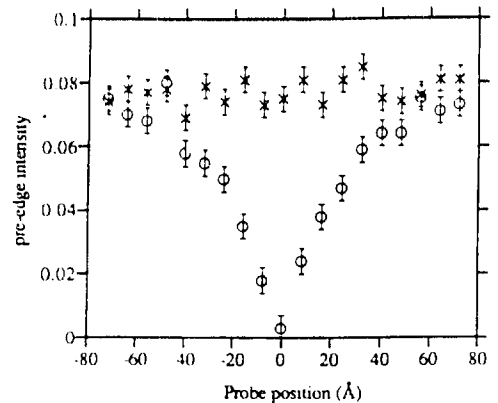36° (near Σ5) boundary showing no
disordered region.

Fig. 7. Hole concentration profiles across
the symmetric (crosses) and asym-
metric (circles) grain boundaries
shown in Fig. 6, obtained by
analyzing the pre-edge feature of
the oxygen K loss. EELS spectra
were recorded every 8 Å with
10 seconds total acquisition time per
spectrum. Note the sensitivity and
spatial resolution obtained at the
cusp, and the lack of hole depletion
at the symmetric boundary.

5. ACKNOWLEDGMENT

6. REFERENCES

[1] S. J. Pennycook and D. E. Jesson, Ultramicroscopy **37**, 14 (1991).
[2] S. J. Pennycook and D. E. Jesson, Acta Metail. Mater. **40**, Suppl. S149 (1992).
[3] S. J. Pennycook and D. E. Jesson, Proc. of Intl. School on Electron Microscopy in
Materials Science (World Scientific Publishing Co. 1992) p. 333.
[4] N. D. Browning, J. Yuan, and C. M. Brown, Physica C **202**, 12 (1992).
[5] N. D. Browning and S. J. Pennycook, Microbeam Analysis (in press 1993).
[6] N. D. Browning, M. M. McGibbon, M. F. Chisholm, and S. J. Pennycook, Proc.
Microscopy Society of America (San Francisco Press), in press 1993.
[7] T. Terashima, Y. Bando, K. Iijima, K. Yamamoto, K. Hirata, K. Hayashi,
K. Kamigaki, and H. Terauchi, Phys. Rev. Lett. **65**, 2684 (1990).
[8] S. J. Pennycook, M. F. Chisholm, D. E. Jesson, D. P. Norton, D. H. Lowndes,
R. Feenstra, H. R. Kerchner, and J. O. Thomson, Phys. Rev. Lett. **67**, 765 (1991).
[9] S. J. Pennycook, M. F. Chisholm, D. E. Jesson, R. Feenstra, S. Zhu, X. Y. Zheng,
and D. H. Lowndes, Physica C **202**, 1 (1992).
[10] S. J. Pennycook, R. Feenstra, M. F. Chisholm, and D. P. Norton, Nucl. Instrum.
Methods Phys. Res. (in press 1993).
[11] S. K. Strieffer et al., Mater. Res. Soc. Symp. **275**, 771 (1992).
[12] N. D. Browning, M. F. Chisholm, S. J. Pennycook, D. P. Norton, and D. H.
Lowndes, Physica C (in press 1993).
[13] S. E. Babcock, X. Y. Cai, D. L. Kaiser, and D. C. Larbalestier, Nature **347**, 167
(1990).
[14] M. F. Chisholm and S. J. Pennycook, Nature **351**, 47 (1991).